Wireless Control of Modular Multilevel Converter Submodules

Barış Çiftçi, *Student Member, IEEE*, Sebastian Schiessl, *Member, IEEE*, James Gross, *Senior Member, IEEE*, Lennart Harnefors, *Fellow, IEEE*, Staffan Norrga, *Member, IEEE*, and Hans-Peter Nee, *Fellow, IEEE*

***Abstract*—Wireless control of modular multilevel converter (MMC) submodules offers several potential benefits to exploit, such as decreased converter costs and ease in converter installation. However, wireless control comes with several challenging engineering requirements. The control methods used with wired communication networks are not directly applicable to the wireless control due to the latency and reliability differences of wired and wireless networks. This article reviews the existing control architectures of MMCs and proposes a control and communication method for wireless submodule control. Also, a synchronization method for pulsewidth modulation carriers is proposed suitable for wireless control. The imperfections of wireless communication, such as higher latency and packet losses compared to wired communication, are analyzed for the operation of MMCs. The latency is fixed with a proper controller and wireless network design. The converter is rendered immune to the packet losses by decreasing the closed-loop control bandwidth. The functionality of the proposal is verified, for the first time, experimentally on a laboratory-scale MMC using a simple wireless network. It is shown that wireless control of MMC submodules with the proposed approach can perform comparably to the wired control.**

***Index Terms*—Distributed control, modular multilevel converter (MMC), prototype, submodule, wireless communication.**

I. Introduction

THE modular multilevel converter (MMC) is the state-of-the-art converter topology for high-voltage and high-power applications [1]. It has been used for more than ten years in high-voltage direct current (HVdc) power transmission systems [2]. HVdc power transmission is advantageous over ac transmission in various technical, economic, and environmental aspects [3]. Technical advantages include the connection of asynchronous ac power systems, ease of long-distance water crossings, and ease of active power control. MMC-based HVdc transmission can provide reactive power to the ac grid and help the power system to operate more effectively. HVdc transmission has lower losses than ac transmission for long lines, and it needs reduced right of way for a certain power. DC cable/overhead line unit cost is less than the ac counterpart. Nevertheless, with today's technology, HVdc terminals that consist of MMCs and ac substations are more expensive than ac transmission terminals with the same power rating. In order to promote the advantages of HVdc transmission further, the MMC costs should be decreased.

The submodules of an MMC need to be switched individually to form the desired output voltage of the converter. In all the internal control methods of MMCs, there is at least one central controller at the top of the control hierarchy, from which all the submodules have a direct or indirect communication link. To the best of the authors' knowledge, this communication system between the central controller(s) and submodules of MMCs has always been realized by using wired communications. An MMC station used for HVdc power transmission may have hundreds of submodules. The submodules may span several hundred meters square, and the total length of the cables used for the communication may sum up to several kilometers. Consequently, the cost of the communication system in an MMC station is high.

The optical fiber cable is the preferred medium in the MMC internal communication system due to its immunity to electromagnetic interference (EMI) and the ability to provide galvanic isolation between the communicating entities. However, it has a high cost and is subject to mechanical stress and fatigue, thus prone to failure. Moreover, the laying out and connection of the optical fiber cables are costly and time-consuming.

Wireless control of the submodules of MMCs is an alternative to remedy the issues mentioned. Especially, for MMCs with high numbers of submodules, it can offer the following advantages:

1) saving the cost of communication cables;
2) saving labor cost of the cabling layout and installation;
3) enabling factory testing and transportation of submodule chains (valves), providing ready-to-operate components;
4) decreasing MMC station installation time;
5) decreasing maintenance time, increasing maintenance period by avoiding the use of optical fiber cable, thus increasing the availability of the MMC station [4].

On the other hand, wireless control of the submodules also brings its own technical challenges and costs. From a technical perspective, wireless communication is stochastic, while wired communication can be regarded as deterministic. When appropriately configured, wired communication is more reliable and has lower latency than wireless communication. Second,

Manuscript received May 23, 2020; revised October 1, 2020 and November 30, 2020; accepted December 14, 2020. Date of publication December 17, 2020; date of current version March 5, 2021. Recommended for publication by Associate Editor M. Saeedifard. *(Corresponding author: Barış Çiftçi.)*

Barış Çiftçi, James Gross, Staffan Norrga, and Hans-Peter Nee are with the KTH Royal Institute of Technology, SE-10044 Stockholm, Sweden (e-mail: bacif@kth.se; james.gross@ee.kth.se; norrga@kth.se; hansi@kth.se).

Sebastian Schiessl is with the u-blox Athens S.A., 15125 Maroussi, Greece (e-mail: sebastian.schiessl9@gmail.com).

Lennart Harnefors is with the ABB Corporate Research, 72178 Västerås, Sweden (e-mail: lennart.harnefors@se.abb.com).

Color versions of one or more figures in this article are available at https://doi.org/10.1109/TPEL.2020.3045557.

Digital Object Identifier 10.1109/TPEL.2020.3045557

wireless communication can be more vulnerable to EMI in an MMC station. Moreover, considering an MMC station as a critical infrastructure, securing its wireless communication network can be more complicated than for a wired network. Similarly, setting up a proper wireless network and placement of the wireless transceivers might be a complicated task considering the safety measures for high-voltage and electromagnetic compatibility. From the expenditure point of view, wireless control requires its own hardware infrastructure. Comparing the hardware costs of the wireless and wired networks for controlling MMC submodules is not meaningful before the technical features of a wireless network that can be used for MMC submodule control are determined. However, there is an increasing demand to control industrial systems wirelessly, possibly leading to a decrease in hardware costs of wireless networks [5].

Wireless control has not been applied for the submodules of MMCs so far. However, it has been used in some other power electronics and power systems applications such as electrical machine drives [6]–[9], battery management systems [10], [11], ac microgrids [12]–[15], and parallel dc–dc [16]–[19] and dc–ac [16], [20] conversions. In electrical machine drives, wireless communication has been mainly used for condition monitoring, fault detection, diagnosis, and estimation. In [6], machine stator current signals, and in [7] and [8], data fusion algorithms applied sensor signals are transmitted wirelessly for condition monitoring and fault diagnosis. In [9], the rotor position of an induction machine is transmitted wirelessly to use in a position-estimation algorithm. In battery management systems, measurements from battery cells, such as voltage, current, internal resistance, and temperature, are transmitted wirelessly to a centralized battery control unit to estimate the state of charge and state of health of the cells [10], [11]. In ac microgrids, wireless communication is used in [12] and [13] to transmit the current references of slave inverters from the master inverter, which is then used for the internal control of the slaves. In [14], the active and reactive power generations of parallel inverters are transmitted wirelessly to enhance the droop control in parallel inverters. Wireless communication is offered for the secondary control, which aims to remove the frequency and voltage deviations in the grid of islanded microgrids in [15]. The use of wireless communication in ac microgrids is related to power system control objectives (grid voltage and frequency control, load sharing) and not similar to the control of MMC submodules, which is for converter internal control. In that sense, parallel dc–dc and dc–ac conversion applications are closer to wireless control of MMC submodules. In the parallel dc–dc and dc–ac conversion applications, either the semiconductor switch ON/OFF signals [16], [17], or the output current references of parallel converters [16], [19], [20], or the insertion indices [18] are transmitted wirelessly. Transmitting ON/OFF signals in [16] and [17] relies on broadcasting on two different radio frequencies, which correspond to the ON and OFF states of the mutual switching signal of parallel converters. The method is not easily scalable to the MMC as each submodule has a different switching pulse pattern and would require a separate transmitter–receiver pair working harmoniously in the presence of other pairs. Further analysis of the wireless transmission of switching signals is presented in Section II-C. Transmitting output current references to the submodules requires each of the submodules to run converter control tasks (detailed in the next section) locally, which is, in general, implemented by the central controller due to the several and complex control objectives of MMCs. Wireless transmission of insertion indices, on the other hand, could be reasonable for the MMC submodules if the indices are transmitted as frequently as the converter control cycle, which is in tens or hundreds of microsecond order, and the switching signals are generated in the submodules.

This article investigates the technical feasibility of the wireless control of submodules in an MMC. The targeted wireless control is related to the internal control of MMCs. For this purpose, a wireless MMC submodule control method based on wireless transmission of insertion indices is proposed. The proposal is analyzed against the latency and packet losses of wireless communication. Wireless control of MMC submodules is verified experimentally on a laboratory-scale MMC for the first time.

The structure of this article is as follows. In Section II, the MMC internal control architectures are reviewed from the wireless control perspective. A wireless control method is proposed in Section III, with a phase-shifted carrier synchronization method suitable for wireless control. Latency and packet losses of wireless communication are analyzed for the operation of MMCs. Section IV includes the implementation details of the proposed method on a laboratory-scale MMC and the experimental results. Finally, Section V concludes this article.

II. MMC Control Architectures and Review for Wireless Control

A. MMC Control System

The MMC topology and its circuit analysis are well documented in the literature [1], [21] and are not repeated in this article. The typical control system of an MMC is shown in Fig. 1. The dashed blocks represent the control layers with their typical cycle times defined by IEEE Standard 1676-2010 for high-power electronics applications [22]. The solid blocks are the main MMC control subsystems [21]. The quantities $i_s^\star$, $v_s^\star$, n, and s represent the converter reference ac-side current, reference ac-side voltage, insertion index, and switching signals, respectively. The control subsystems are fed back with the variables shown below them. The system control and application control are the high-level control layers connected to the power system that governs the MMC. The output current control is the heart of the converter control layer, which fundamentally determines the operating point of the MMC in its power range. The arm-balancing control ensures equal total stored energy in the upper and lower arms and regulates the circulating currents. According to the switching signals generated by the modulation control and submodule capacitor voltage control, a submodule of the MMC is inserted to or bypassed from the arm circuit.

B. MMC Internal Control Architectures

There are three main MMC internal control architectures in the literature: centralized, decentralized, and distributed. These architectures are also practiced in ac microgrid applications [23]–[26]. Nonetheless, the definitions of decentralized

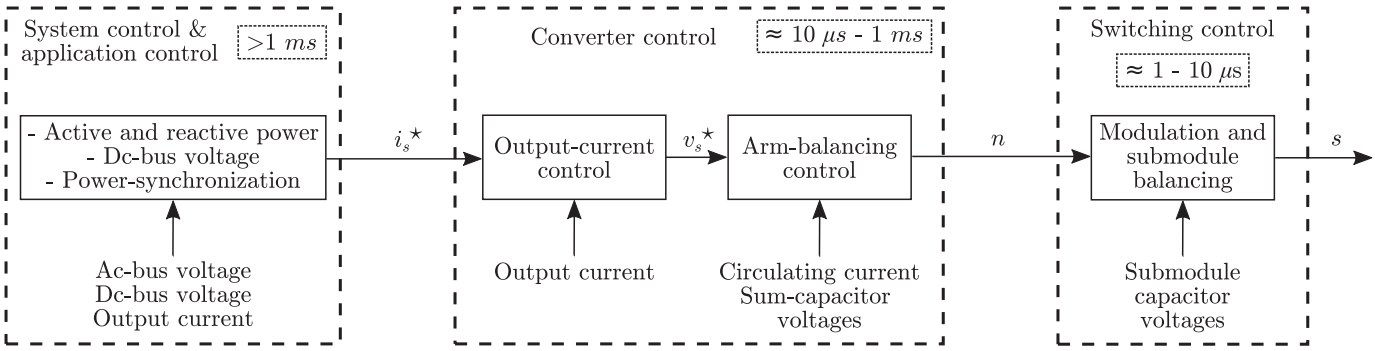

Fig. 1. Block diagram of the typical control system of an MMC. The dashed blocks represent the control layers with their typical cycle times defined by [22]. The solid blocks are the main MMC control subsystems [21] fed back with the variables shown below them.

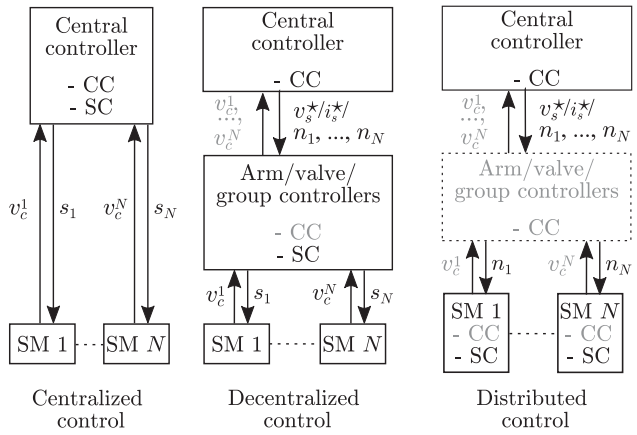

Fig. 2. Three main internal control architectures of MMCs. CC and SC stand for converter control and switching control, respectively.

and distributed architectures differ in ac microgrid applications from their definitions in MMC internal control applications. In ac microgrids, there is no central controller in the decentralized and distributed control. The microgrid components communicate with each other in distributed control via a (low-bandwidth) wired or wireless network, whereas in decentralized control, all the microgrid components operate on their own with their local variables. In the next paragraphs, the decentralized and distributed control architectures in MMC internal control applications are explained, followed by the rest of this article for consistency with the literature.

The control architectures are illustrated in Fig. 2. CC and SC stand for converter control and switching control, respectively, and v_c^i, s_i, and n_i are the capacitor voltage, switching signal, and insertion index of the ith submodule, respectively. The gray variables and dashed block correspond that they may exist or not depending on the implementation. In the centralized architecture, after receiving $i_s^\star$ from a high-level controller, all the control subsystems related to the converter control and switching control layers are run in a single central controller, and the switching signals are transmitted directly to each submodule [1]. If the processing capabilities, the available number of input/outputs, or the communication bandwidth of the central controller are not sufficient, centralized control can be expanded to multiple control layers [27], [28], and called as decentralized control [28]. In these cases, the mentioned control tasks are hierarchically structured and shared between a central controller located at the top and several arm/valve/group controllers below that (the arm/valve/group controllers can be in hierarchical order). Modulation is done in the arm/valve/group controllers, and the switching signals are transmitted to the submodules. There is no need for an advanced controller in the submodules in both the centralized and decentralized control architectures.

Alternatively, in distributed control architecture, the submodules have their controllers taking part in the MMC control tasks. The arm/valve/group controllers may exist between the central controller and the submodules or not. Assuming they do not exist, the central controller and the submodule controllers work in the master–slave configuration. The converter control and switching control tasks can be allocated to the central controller and the submodule controllers in various ways. In [29] and [30], local stationary frame current regulators are used in the submodules, assigning the converter control layer and switching control layer tasks to the submodules. Although work [30] defines its control architecture as decentralized, since the submodules take part in the control of the MMC with their own controllers and they are connected to the master controller with no other control layer in between, it is categorized as a distributed architecture as the majority of the other literature with similar architectures [29], [31]–[35]. Specific control objectives related to converter and switching control layers are assigned to two submodule groups with different controller designs in [31]. In the most widely used distributed control architecture, the converter control layer is performed by the central controller, and the switching control layer is performed by the submodule controllers [32]–[35]. This configuration enables the use of identical submodules with reduced internal communication requirements when the transmission of submodule capacitor voltages is avoided [34], [35], and the use of a relatively low-bandwidth network between the central controller and the submodules. Modulation in the distributed architectures is most widely realized by carrier-based modulation methods: phase disposition [30] and especially phase-shifted modulation [29], [31]–[35]. It is important to note that, in centralized and decentralized control, the modulation is done out of the submodule controllers, and in distributed control, it is done in the submodule controllers.

C. Review of Control Architectures for Wireless Control

The control of MMCs is a time-critical process. The data exchange between control algorithms of MMCs requires low latency and high reliability. Considering the stochastic nature of wireless communication, excessive latency or consecutive loss of wirelessly transmitted data can lead to various problems, such as harmonic distortion, overvoltages, overcurrents, and instability. Thus, a communication scheme, in which the delays and losses are minimized, should be designed along with a control system that can cope with these concerns. To reduce the risks, the amount of data that need to be transmitted wirelessly should be decreased, and their period of transmission should be increased in both directions of the communication between the central controller(s) and submodules. The control architectures are reviewed in the next paragraphs from these perspectives.

If a centralized or decentralized architecture is to be used for wireless control, first of all, the switching signals (s in Fig. 1 and $s_{1/N}$ in Fig. 2) have to be transmitted wirelessly from the central or arm/valve controllers to the submodules. The switching states are tightly scheduled. The delay or loss of them can quickly cause problems ranging from distortions of the generated voltage to overcharge or discharge of the submodule capacitors and loss of stability. Even if the transmission is assumed to be ideal, centralized and decentralized control is problematic from the scheduling point of view, particularly if carrier-based modulation is used. As an example, for a three-phase MMC with 100 submodules per arm and fundamental switching frequency (which is the lowest meaningful value that can be used [36]), there is a need for switching in one of the submodules approximately every 15 μs. As a switching need arises, the command either should be transmitted immediately, or several of them should be delayed, grouped, and transmitted periodically. The former method provides the ideal synthesis of the output voltage. However, performing wireless transmission with such small intervals is a very demanding task. The latter method enables to use a single broadcast channel, and the transmission interval can be adjusted according to the capabilities of the wireless network. Still, the synthesized voltages are not ideal anymore. Thus, it can be concluded that wireless control using a centralized or decentralized architecture is not feasible.

If a distributed control architecture with a phase-shifted carrier-based modulation is to be used for wireless control, the insertion indices (n in Fig. 1 and $n_{1/N}$ in Fig. 2) have to be transmitted wirelessly. From the output current control and arm-balancing control points of view, the same insertion index is valid for all the submodules of an MMC arm. The indices might be adjusted for individual submodule capacitor voltage control purposes, which are performed in the submodule controllers. Thus, there are six insertion indices for the six arms of the MMC to transmit from the central controller. The length of this primary payload is fixed and independent of the number of submodules. If the insertion indices are put in a single data packet, they can be broadcast to all the submodules periodically. This approach dramatically relaxes the scheduling and required data rate of the wireless transmission. The wireless data may still be delayed or lost, but the modulation and switching can continue in the submodules, which are vital for the operation of MMC, especially in fault cases. In case of transmission errors for some or all submodules, submodule controllers can either continue modulation with the previously received indices or generate their own indices until the communication recovery. For this purpose, the previously received data and the local variables (capacitor voltage, if available, arm current) of the submodule can be utilized. The measures to take and the design of algorithms during such errors form a distinct research subject, which can be called the autonomy of submodules, and is not covered further in this article.

III. Structure and Analysis of the Proposed Wireless Control Method for MMCs

In light of the discussion in the previous section, the distributed control architecture using a two-level hierarchy with phase-shifted carrier-based modulation is convenient for wireless control of MMC submodules. The ac-side (output) current, arm balancing, and any other upper-level control tasks are performed by the central controller, whereas modulation and submodule capacitor voltage control are performed by the submodule controllers. All the central and submodule controllers should have wireless communication infrastructure, preferably on the same board/platform that the control algorithms executed. The insertion indices of all converter arms should be periodically broadcast in a single data packet. The wireless transmission cycle should be set equal to the sampling period of the central controller.

The ac-side current control of MMCs can be realized with different methods such as proportional-resonant (PR) controllers for single-phase MMCs or vector current controllers for three-phase MMCs [21]. Similarly, the circulating current control, which is a part of the arm-balancing control, can be realized with a PR controller or a vector current controller in single- or three-phase MMCs, respectively. The ac-side and circulating current controllers require the arm current measurements. Also, the point of common coupling (PCC) voltage measurements are required for phase-locked loop and for feedforward control in the ac-side current controller. In each sampling period, these measurements should be fed back to the central controller. The number of measurements to feed back is low and independent of the number of submodules. On the other hand, the excessive delay or loss of these measurements could lead to stability problems in the ac-side or circulating current controllers. Thus, there is not much to gain when the measurement feedback paths are made wireless, even leading to complications. Consequently, the arm current and PCC voltage measurements are advised to feed back via a wired network.

The choice of arm-balancing control requires attention. The obligate payload from the submodules to the central controller (uplink data) for the steady-state operation of the MMC depends on the chosen method for arm-balancing control and submodule capacitor voltage control. Some of the arm-balancing control methods require submodule capacitor voltage measurements (closed-loop control [37] and hybrid control [21]). However, the transmission of such a large amount of data, which increase with the number of submodules, burdens the wireless network from the bandwidth and scheduling points of view. Thus, it is

wise to use a control method that does not rely on capacitor voltage measurements. Direct voltage control (also known as direct modulation) and open-loop voltage control [38] are of this kind. In this article, open-loop voltage control is preferred, since it provides lower parasitic voltage components on the ac-side and internal voltages [21]. The block diagram of open-loop voltage control is shown in Fig. 7 with other central controller components, which will be detailed in Section IV.

As expressed previously, carrier-based modulation, especially the phase-shifted modulation, is the most widely used modulation method in distributed control applications. This choice is also reasonable from the wireless control perspective. Provided that the switching frequency of the submodules is not an integer multiple of the fundamental frequency, phase-shifted carrier-based modulation ensures reasonably well-balanced capacitor voltages without requiring capacitor voltage measurements or insertion/bypass states of other submodules [39]. Otherwise, the methods that require these data, such as capacitor voltage sorting based algorithms, pose further tasks that grow with the number of submodules on the communication system. On the other hand, a well-known issue of carrier-based modulation in distributed MMC control applications is the asynchrony of carriers generated in submodule controllers [30], [32]–[35], [40], [41]. The challenge and proposed solution are detailed in the next subsection.

Considering all the proposed control loops in the central controller and submodules, there is no imperative uplink data from the submodules to the central controller for the steady-state operation. Nonetheless, auxiliary signals (submodule capacitor voltages, temperatures, and semiconductor states) from the submodules may need to be sent back to the central controller for fault identification and handling. However, this article does not consider fault handling, and these possible uplink signals are, therefore, disregarded in the wireless network. Hence, a simple, unidirectional, broadcast-type wireless transmission is sufficient for the steady-state operation. The architecture of the proposed control method is shown in Fig. 3. The quantities $i_{ua,b,c}$ and $i_{la,b,c}$ are the instantaneous values of the upper and lower arm currents, respectively, and $i_{sa,b,c}$ are the instantaneous values of the ac-side currents. L is the arm inductor. The architecture is generic and can be applied to MMCs with any submodules per arm with the same wireless payload.

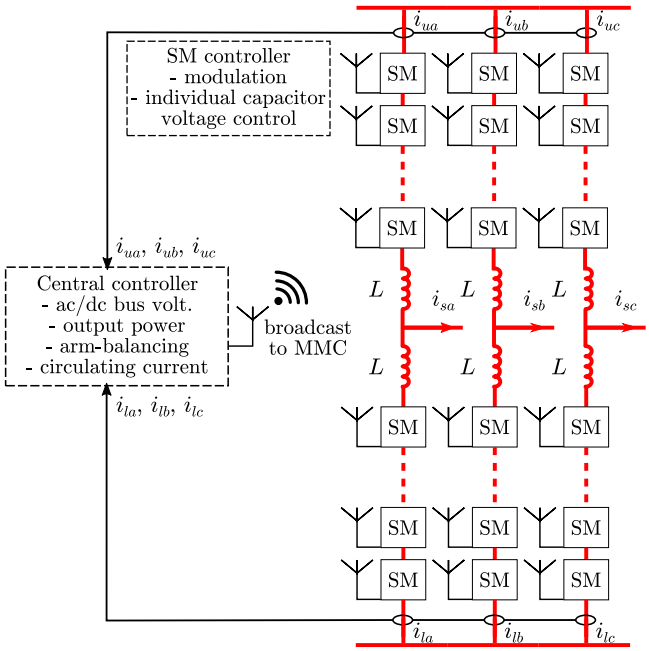

Fig. 3. Architecture of the proposed wireless MMC submodule control.

A. Asynchrony of Phase-Shifted Carriers and Proposed Synchronization Method

In a centrally controlled MMC, the required phase shifts between the modulation carriers can be set with high precision since one and the same hardware generates them. On the other hand, the carriers generated in submodule controllers have the problem of drifting away from each other because of the different frequency tolerances of individual crystal oscillators, which source the counters that generate the carriers. This difference causes the carriers to have slightly different frequencies than the target. The frequency differences integrate over time and result in distorted phase shifts. The most significant effect of the distortion on MMC operation is the undesired generation of low-frequency harmonics on the odd integer multiples and around all the integer multiples of carrier frequency f_c [42], [43]. The amplitudes of these low-frequency harmonics are proportional to f_c, frequency tolerance of the clock sources, and the integration interval. For this reason, the carriers in the submodule controllers need to be synchronized periodically before the consequences of asynchrony become detrimental. Synchronization of distributed carriers is discussed for several wired networks, most of which propose the use of special synchronization functions of field-bus networks such as EtherCAT [34], [40], [41] or CAN [32], [33], or propose periodic transmissions only for synchronization purpose [30], [35].

The synchronization should, ideally, reset all the asynchrony and provide the exact required phase shift. However, especially in a wireless control environment, the synchronization may be imperfect due to the delays and losses of the synchronization signal, resulting in an unavoidable asynchrony. Thus, the wireless control method should provide a robust and straightforward synchronization mechanism with satisfactory performance. This article proposes the following synchronization method for wireless control of MMC submodules.

1) The phase-shifted carrier period is set as an integer multiple (i.e., p times) of the wireless transmission period.
2) The wireless payload sent from the central controller contains a 1-bit synchronization flag.
3) In every pth wireless transmission, the flag is set.
4) Submodule controllers reset their carriers to the initial phase shifts as soon as they receive the wireless data with the synchronization flag set.

The method requires only 1 bit for the synchronization of all the submodules. As it is embedded in the periodic wireless data packet, there is no additional scheduling and transmission task. Carriers are synchronized at every period. The synchronization precision is only dependent on the wireless data reception time spread of submodules, assuming that the internal processing

times of the submodules are the same. For the broadcast type of wireless data, the reception time is approximately equal for all submodules. The only source of reception time difference is the propagation delay of the broadcast data over the air. For example, the data reception time difference between two submodules placed a couple of hundred meters away from each other is in the submicrosecond range. Then, the unavoidable asynchrony is less than 0.1% of the full period for a 1-kHz carrier. The experimental performance of the proposed synchronization method can be observed in Section IV-E.

B. Wireless Communication Network

Time-critical applications do not have a generally accepted and mature wireless communication standard. In the wireless control of MMC submodules, a definite number of transceivers are fixed in the space. They do not have power constraints. With the proposed control method, the payload to transmit is in the range of tens of bits in every sampling period (typically 100 μs). The transmission is unidirectional and of broadcast type. There is no retransmission. In this article, the functionality of the proposed control method is intended to be observed with an elementary wireless network. For this aim, the IEEE 802.11a Wi-Fi protocol [44] with only the physical layer (but no other network layers) is considered. The resultant network provides no extra measures to increase the reliability and forms merely a basis for the wireless control performance of the MMC submodules.

C. Analysis of Latency in Wireless Control

The components that contribute to total time delay T_d of the control system in an MMC are [45] the following:

1) sampling delay T_{ADC};
2) controller delay T_{DSP};
3) communication delay T_{COM};
4) pulsewidth modulation (PWM) delay T_{PWM}.

The characteristics of these components are explained in the referred article and not repeated here. However, the sampling techniques and the related controller delay should be reconsidered. In two-level converters controlled by standard microcontrollers or digital signal processors (DSPs), the sampling of voltages and currents is synchronized with the carriers such that the sampling is performed at the peak and/or valley of the carriers. The reference in the modulation stage is updated only at the sampling instants. In this way, no low-frequency aliasing errors occur in the sampled signal spectrum even if no antialiasing filter is used. However, it results in fixed controller delays of either full or half the sampling period [46]. From the control perspective, the total time delay should be minimized. Minimization of time delay is even more critical for control systems with wireless communication, which may have longer and random delays than wired communication. Thus, it makes sense to reduce the full or half sampling period controller delay. Indeed, synchronization of sampling and modulation does not make sense in MMCs with phase-shifted carrier-based modulation in terms of avoiding low-frequency aliasing errors. Considering a single submodule of an arm with N submodules, its modulation is synchronized with the sampling instant(s) corresponding to its own carrier. Still, all the other $N-1$ submodules can be at any point during their modulation period. Thus, the motivation for avoiding switching harmonics in the sampled signal is not valid. However, this asynchrony does not give rise to significant problems if the sampling frequency is sufficiently high such that the spectrum of the sampled signal is negligible above the Nyquist frequency. This, in fact, is the case where the equivalent switching frequency is Nf_c or $2Nf_c$, and owing to the arm inductors, the switching harmonics in this frequency range become negligible. Therefore, it is no longer required to synchronize sampling with modulation and delay the insertion index update until the next sampling instant. The immediate update enables a smaller system time delay, which is advantageous to compensate for the wireless communication delays.

Any latency originating from the wireless control can be added to T_{COM}. The components that contribute to T_{COM} in a wireless network can be categorized as:

1) processing delay;
2) transmission delay;
3) propagation delay.

Processing delay is the time taken by the transceivers to process the data packet for wireless transmission or reception. It also includes the queuing delay for transmission, which is when the wireless packet spends before accessing the transmission medium. Transmission delay is the time required to push all the wireless packet bits into the transmission medium. It is a function of the number of bits P and the data rate R and can be approximated as P/R, excluding some fixed-size overhead. Propagation delay is the time it takes for the first bit of the wireless packet to travel from the transmitter to the receiver. It is a function of the propagation speed (speed of light, c) and the distance to be traveled d, and is d/c.

The simple wireless network proposed in the previous section only uses the physical layer of the IEEE 802.11a standard. The transmission relies on broadcasting periodic and fixed-length data from the central controller to receivers at fixed locations in a dedicated channel only accessed by the central controller. Hence, the transmission delay is fixed and the same for all submodules. The propagation delays are fixed for each submodule but have a variance between each other at most in the submicrosecond range, as explained in Section III-A. Since having periodic and fixed-length data, the processing delay can be regarded as fixed, too. The amount of the data are sufficiently small to finish the transmission before the next data packet is formed. Therefore, transmissions can start immediately when new data are present. As a result, there is no queuing delay. Considering all the above, in the proposed wireless network, one can expect no random latency in the received data if the data reception is successful. On the other hand, transmission errors can still occur since wireless channels are subject to fading, noise, and interference. Consequently, the considered wireless network results in two cases for the reception: 1) the data are received with no random delay but with deterministic delays, as explained above; and 2) the data are lost. The effects of these highly deterministic latencies and random packet losses should be evaluated for the MMC controllers.

The most important effect of latencies is the decreased phase margin in closed-loop control. Extreme latencies can cause

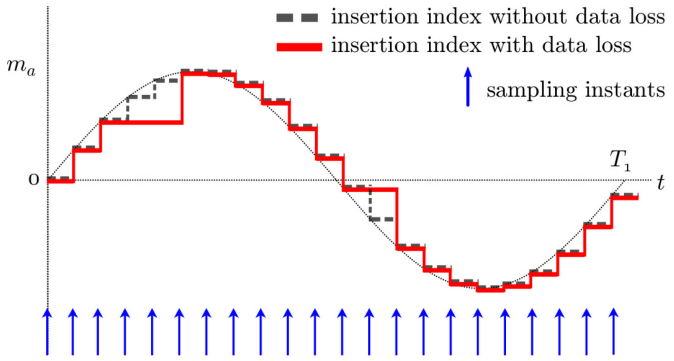

Fig. 4. Received insertion indices by the submodules with and without packet losses in wireless communication.

instability. The stability of the converter should be assessed with the calculated/measured total latency and the parameters of the controllers and converter. The assessment is exemplified in Section IV-D.

D. Analysis of Packet Losses in Wireless Control

In a wireless communication network, the length of packet loss trains depends on several factors, including the employed communication protocol, the environment in which the communication is conducted, time, geographical position, the distance between the transceivers, packet size, and more. A common method of characterizing communication networks in wireless control applications is to do measurements in the targeted industrial environment [47]. In this way, while mimicking the communication required for wireless control, several network parameters can be obtained, such as the distribution of packet losses length, the mean, standard deviation, and maximum of them.

The submodule controllers can be designed to update the insertion index in their modulation process with the received data if they receive a wireless data packet. Otherwise, they continue to use the last successfully received insertion index. In Fig. 4, the insertion indices received by the submodules are illustrated with random losses and without loss of the wireless packets. m_a is the modulation index and T_1 is the fundamental period. In the control algorithms of MMCs, the packet loss can be modeled as a decrease in the sampling frequency for the period of packet loss. The MMC can be rendered immune against the majority of the packet losses by taking the duration of the longest "tolerable" packet loss train as the longest sampling time and tuning the controller accordingly. In other words, the controller can be designed with a lower sampling frequency considering the packet loss trains but operated with a higher sampling frequency to provide room for losses. This approach disregards the packets received more frequently than the corresponding frequency of considered packet loss train. Hence, it provides a worst-case scenario as if the considered packet loss train occurs periodically. In an MMC with no loss of control data and with a PR or proportional-integral current controller, the sampling frequency ω_s and desired closed-loop-system bandwidth α_c are related as [21]

$$\alpha_c \leq \frac{\omega_s}{10} \tag{1}$$

where ω_s is defined as

$$\omega_s = \frac{2\pi}{T_s} \tag{2}$$

and T_s is the sampling period. Then, if the considered tolerable packet loss train lasts k consecutive sampling intervals, the desired closed-loop bandwidth should be decreased to

$$\alpha_c \leq \frac{\omega_s}{10(k+1)} \tag{3}$$

to render the MMC immune against a maximum of k consecutive packet losses. The tolerance to consecutive packet losses is related to the bearable decrease in the desired closed-loop control bandwidth. The excessive bandwidth reduction is not desirable, and the minimum bearable bandwidth is dependent on the specific application. Then, there would be packet loss trains to which the MMC controllers are not tuned for. The methods to deal with these long packet losses and continue the regular operation of MMC or the methods to mitigate the detrimental effects of abnormal operation during long packet loss trains are out of the scope of this article. However, the consequences of these long packet loss trains are exemplified experimentally in Section IV-E.

TABLE I
MMC PARAMETERS

	Symbol	Value
Fundamental frequency	ω_1	$2\pi 50$ rad/s
Pulse number (frequency ratio)	m_f	16.67
Submodules per arm	N	3
Offset between upper and lower arm carriers	$\beta^\dagger$	0 rad
Frequency tolerance of FPGA clocks	$\Delta f/f_{\text{osc}}$	50 ppm
Dc-side voltage	V_{dc}	100 V
Modulation index	m_a	0.95
Ac-side resistance	R_o	10.0 Ω
Ac-side parasitic inductance	L_o	0.200 mH
Arm parasitic resistance	R	0.3 Ω
Arm inductance	L	1.185 mH
Submodule capacitance	C_{sm}	2.7 mF
Dc-side capacitance	C_{dc}	1.0 mF

†The value of β with odd N results in having the first group of switching harmonics around $2Nf_c$.

IV. IMPLEMENTATION OF WIRELESS CONTROL AND EXPERIMENTAL RESULTS

The wireless control method proposed in Section III is implemented on a single-phase laboratory-scale MMC [48] to validate its viability and evaluate its performance. The wireless control performance is benchmarked against that of the wired control featuring the same control algorithms. The parameters of the MMC are given in Table I. The phase-shifted carrier period is set 12 times the wireless transmission period (which is equal to the inverse of the sampling frequency given in Table II), making the pulse number equal to 16.67. Three submodules are used per arm, enough to obtain the multilevel voltage characteristics while enabling rapid prototyping. The modulation index is high at 0.95, as in HVdc transmission applications.

TABLE II
CONTROLLER PARAMETERS

	Symbol	Value
Sampling frequency	ω_s	$2\pi 10$ krad/s
Closed-loop-system bandwidth of the ac-side-current controller	α_c	$\frac{\omega_s}{10(k+1)}$ [rad/s]
Proportional gain of the ac-side-current controller	K_p	$\alpha_c L/2$ [Ω]
Bandwidth of the ac-side-current resonant controller	α_1	$\alpha_c/10$ [rad/s]
Resonant gain of the ac-side-current controller	K_1	$\alpha_1\alpha_c L$ [Ω/s]
Virtual resistance of circulating-current controller	R_a	$\alpha_c L/2$ [Ω]
Bandwidth of the circulating-current resonant controller	α_2	50 rad/s
Resonant gain of the circulating-current controller	K_2	100 Ω/s
Bandwidth of the open-loop voltage controller band-pass filter	α_f	31 rad/s
Proportional gain of the individual submodule-capacitor-voltage controller	G_0	0.2
Ac-side current maximum peak value	$\hat{I}_{\max}$	8 A

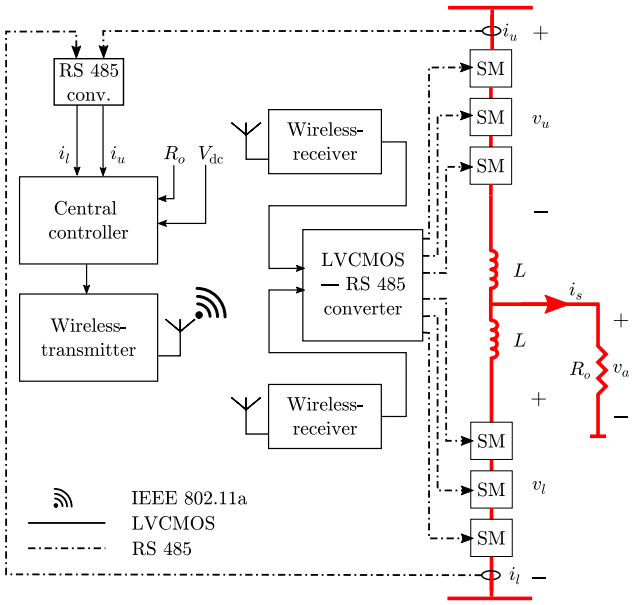

Fig. 5. Structural diagram of the wirelessly controlled single-phase MMC experimental setup. The payload of wireless packets is shown in Fig. 8. R_o and $V_{\rm dc}$ are provided to the central controller by the operator.

The same submodules of the MMC in [48] have been used while keeping the same submodule capacitance, which is a bit high for the operating conditions in this article. However, the high capacitance value does not have any effect on the wireless submodule control. On the other hand, the arm inductance is lower than the original design, making the internal control more difficult. The MMC consists of half-bridge submodules and is operated in the inverter mode. The structural diagram of the setup is shown in Fig. 5. i_u, i_l, and i_s are the upper arm, lower arm, and ac-side currents, respectively; v_u, and v_l are the inserted upper arm and lower arm voltages of the MMC, respectively; and v_a is the voltage over ac-side resistance, ac-side voltage v_s is equal to $(-v_u + v_l)/2$. There are three wireless transceivers: one connected to the central controller working as a transmitter and one receiver for each upper and lower MMC arms. The separation of controller and transceiver boards, consequently the use of RS 485 physical layer between these boards, and the use of one wireless receiver per arm are special conditions of the setup compared to the proposal given at the beginning of Section III and illustrated in Fig. 3. The separation of controller and transceiver boards causes board-to-board communication delays (detailed in Section IV-D) compared to when the controller and transceivers are on the same platform but possibly separate chips. On the other hand, using a single receiver per arm does not affect the control algorithms or parameters compared to the original proposal. Moreover, it does not have a distinguishable effect on the experimental results of this article, which is verified by simulation studies but not shown due to the length of the article. In the wired control case, the central controller is connected directly to the LVCMOS—RS 485 converter in Fig. 5. The components of the setup are explained in Sections IV-A–IV-C. Latency analysis of the setup is given in Section IV-D, and the experimental results are given in Section IV-E.

A. Central Controller

The central controller is a Xilinx Zynq-7000 SoC ZC702 Evaluation Kit. During every sampling period, it executes the following tasks sequentially:

1) sampling the arm currents with wired communication;
2) running ac-side current, circulating current, and arm-balancing controllers;
3) generating the insertion indices and forming up the wireless payload;
4) transferring the wireless payload to the attached wireless transmitter.

PR controllers are used as the ac-side and circulating current controllers, and the open-loop voltage controller is used for the arm-balancing control. v_a is fedforward in the ac-side current controller to improve its dynamic performance. The block diagrams of the controllers with their respective plants and T_d are shown in Fig. 6. In the ac-side current control loop, $i_s^\star$ is the reference ac-side current, K_p and K_1 are the proportional and resonant gains of the ac-side current controller, respectively, $v_s^\star$ is the ac-side voltage reference, and v_a^f is the feedforward voltage of the ac-side resistance, which is defined as

$$v_a^f = \frac{V_{\rm dc}}{2} m_a \sin \omega_1 t. \tag{4}$$

In the circulating current control loop, $i_c^\star$ and i_c are the reference and instantaneous circulating currents, respectively, K_2 and R_a are the resonant gain and the virtual resistance of the circulating current controller, respectively, and $v_c^\star$ is the internal voltage reference. The central controller block diagram is shown in Fig. 7, where $v_{cu}^{\Sigma\star}$ and $v_{cl}^{\Sigma\star}$ are the sum capacitor voltage estimates for the upper and lower arm, respectively, and $synch$ is the synchronization flag. The controller parameters are listed in Table II as a function of k in (3). The parameters are chosen according to the MMC controller design suggestions in [21]; the design processes are not repeated for brevity. The stability analyses of the controllers are conducted in Section IV-D. The central controller forms the wireless data packet and sends it immediately to the wireless transmitter to be broadcast. Asynchronous

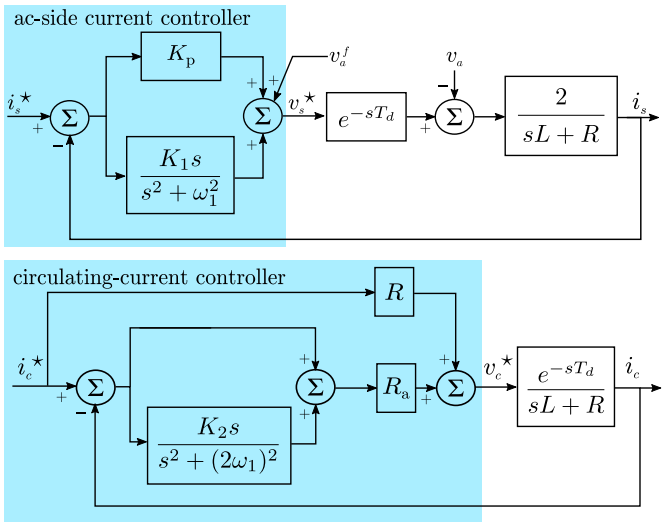

Fig. 6. AC-side current (upper) and circulating current (lower) control loops. i_s and i_c are calculated from the wired $i_{u,l}$ measurements, as shown in Fig. 5.

serial communication with 480-ns bit length (2.08 Mbit/s) is used between the central controller and the wireless transmitter. A diagram presenting the data packet sent from the central controller is shown in Fig. 8 . The packet is structured as if the MMC were a three-phase converter to obtain the worst-case latency. Apart from the insertion indices and the carrier synchronization flag, the packet contains arm currents, dc-bus voltage, and a proportional gain to use in individual capacitor voltage control, which is detailed in the next subsection.

B. Submodule Controllers

The submodule controllers are DIPFORTy1 Soft Propeller modules equipped with a Xilinx Zynq-7 XC7Z010 system on a chip. They are connected to the wireless receivers with the same parameters as the central controller wireless transmitter communication. The block diagram of the submodule controllers is shown in Fig. 9, where $v^\star_{cu,l}$ and $v^i_{cu,l}$ are the reference and instantaneous submodule capacitor voltages, respectively, n_cap is the individual capacitor voltage control term, n_i and s_i are the insertion index and the switching signal of the submodule, respectively. Individual submodule capacitor voltage control is added as a secondary submodule-capacitor-voltage-balancing control [21]. In this control, G_0 is the proportional gain, and $\hat{I}_\mathrm{max}$ is the maximum allowed ac-side current peak value. If there is no current sensor on the submodules, which might be the case due to its cost, the arm current measurement and the reference capacitor voltage should be transmitted from the central controller. These two groups of downlink data can be attached to the insertion indices and broadcast together, as shown in Fig. 8. The arm current measurements received by the submodules have the wireless communication delay as extra compared to the measurements received by the central controller. Since the sign of the arm current affects the sign of n_cap, the extra delay can cause degradation on the individual capacitor voltage control performance near the arm current zero crossings. On the other hand, n_cap is almost zero near the arm current zero crossings. Thus, the degradation is insignificant. The submodule controllers execute the following tasks concurrently:

1) receiving the payload of the central controller (see Fig. 8) via the wireless receivers;
2) calculating the individual submodule capacitor voltage control reference (n_cap in Fig. 9);
   a) sampling the submodule capacitor voltage with $2f_c$ sampling frequency;
3) modifying the received insertion index with the individual submodule capacitor voltage control reference;
4) resetting the carrier to the initial phase if the synchronization flag is set in the received payload;
5) phase-shifted carrier-based PWM.

The phase and frequency of the carriers are fixed in the embedded software.

TABLE III
WIRELESS COMMUNICATION PARAMETERS

Protocol	IEEE 802.11a
Data rate	18 Mbit/s
Modulation	QPSK
Payload	32 B
Transmission power	10 dBm

C. Wireless Transceivers

The wireless transceivers are based on a WARP v3 Kit. WARP project offers a reference IEEE 802.11 orthogonal frequency-division multiplexing physical layer (PHY) and a distributed coordination function medium access control (MAC) design for the WARP v3 Kit. In this study, carrier-sense and random backoff mechanisms of the MAC layer are disabled, and PHY is used for wireless networking. As soon as the wireless transmitter receives the data packet in Fig. 8 from the central controller, it broadcasts the packet after adding the 8 B header and 4 B frame check sequence. The wireless receivers forward the payload of the central controller to the submodule controllers when they receive a wireless packet successfully. The parameters of the wireless transmission are listed in Table III. It is important to note that the experiments are conducted in an indoor laboratory in the basement with low transmission power. Any other Wi-Fi device in the vicinity does not use the wireless channel used in the experiments. Therefore, no substantial harmful interference with other devices is created.

D. Latency Analysis of the Setup

The delay components listed in Section III-C have been measured and calculated for the experimental setup. The following values were obtained.

1) T_ADC was measured to be 3.51 μs (including the wired communication between the current sensors and the central controller).
2) T_DSP was measured to be 4.91 μs.
3) T_COM:
   a) serial communication delay from the central controller to the wireless transmitter was calculated as

$$T_\mathrm{srl} = 480\,\mathrm{ns/bit} \cdot 136\,\mathrm{bits} = 65.28\,\mu\mathrm{s} \quad (5)$$

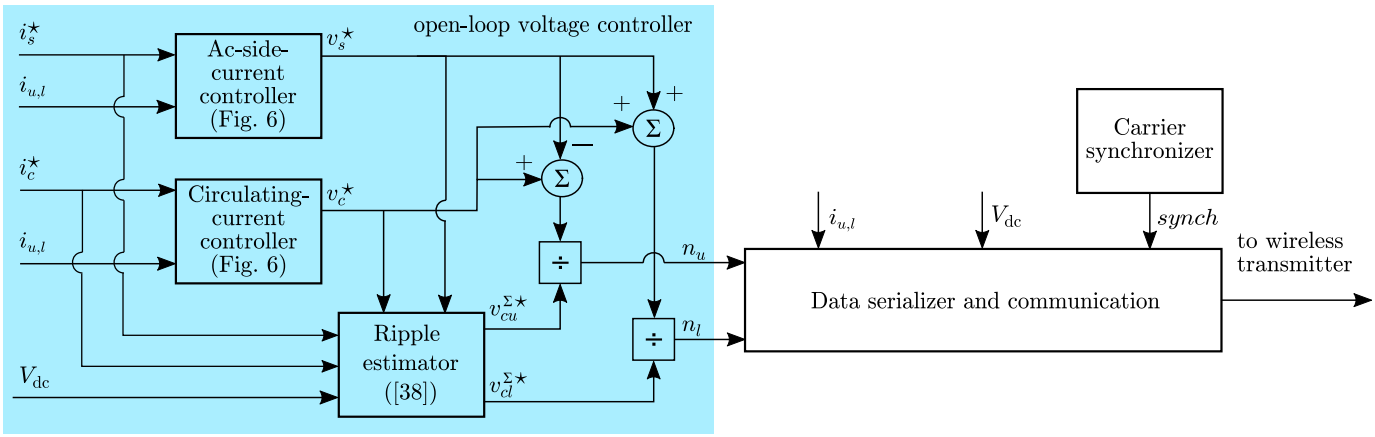

Fig. 7. Central controller block diagram of the experimental setup. $i_s^\star$ and $i_c^\star$ are calculated internally using $V_{\rm dc}$ and R_o that are provided by the operator, and $i_{u,l}$ are obtained from wired measurements, as shown in Fig. 5. *synch* is generated internally.

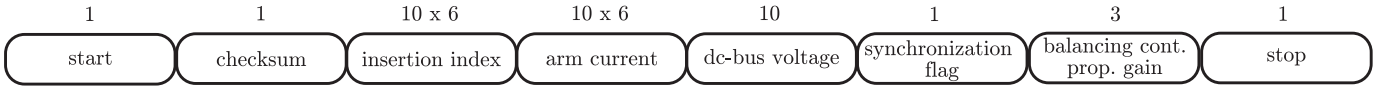

Fig. 8. Payload of the central controller to be sent wirelessly with the corresponding number of bits on top. Multiplication with 6 represents the data of the six arms of the MMC.

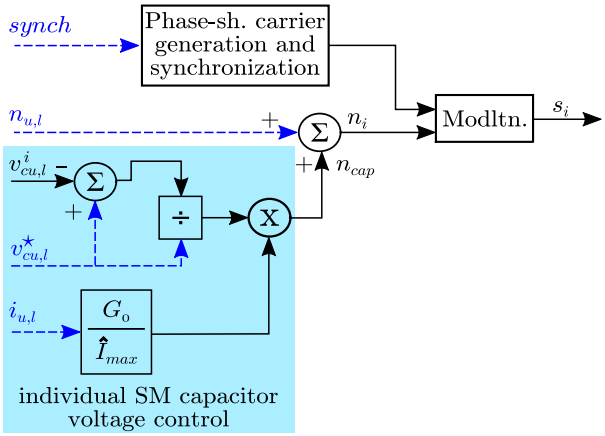

Fig. 9. Submodule controller block diagram of the experimental setup. The dashed inputs in blue are wirelessly received, and $v_{cu,l}^i$ is measured locally. $v_{cu,l}^\star$ is equal to $V_{\rm dc}/N$.

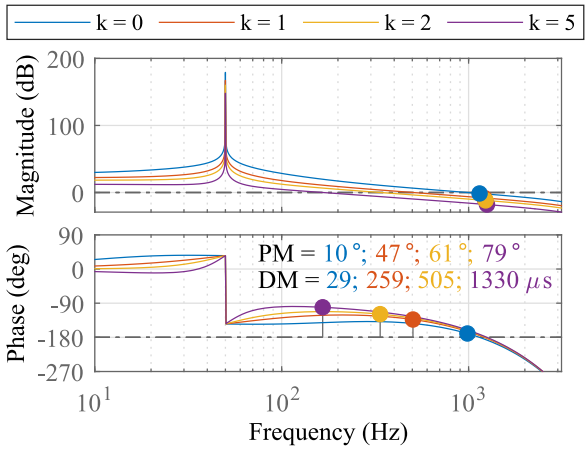

Fig. 10. Bode plot of the ac-side current control open-loop transfer function.

b) wireless transmission delay $T_{\rm wrlss}$ from wireless transmitter serial input pins to wireless receiver serial output pins was measured to be 52.95 μs;
c) serial communication delay from the wireless receivers to the submodule controllers is the same as (5).

4) $T_{\rm PWM}$ is calculated based on multisampled PWM delays [49] as

$$T_{\rm PWM} = \frac{T_c}{2\dfrac{f_s}{f_c}} = \frac{1}{2f_s} = 50\,\mu{\rm s} \tag{6}$$

where T_c is the carrier period and f_s is the sampling frequency. Consequently, T_d is equal to the sum of the delays above and calculated as 241.93 μs for wireless communication. This delay is highly deterministic with the proposed control and communication methods. The open-loop transfer functions of the ac-side and circulating current control loops can be obtained from Fig. 6 as

$$G_{\rm ac}(s) = \frac{2[K_p(s^2+\omega_1^2)+K_1 s]}{(s^2+\omega_1^2)(sL+R)}e^{-sT_d} \tag{7}$$

$$G_{\rm cc}(s) = \frac{(R_a+R)[s^2+(2\omega_1)^2]+R_aK_2\,s}{[s^2+(2\omega_1)^2](sL+R)}e^{-sT_d} \tag{8}$$

respectively. Then, the Bode diagrams of the open-loop transfer functions can be analyzed to determine their closed-loop stability. Bode diagrams with different k values and above-defined T_d are obtained as in Figs. 10 and 11. In the figures, PM and DM stand for the phase and delay margin, respectively. The control

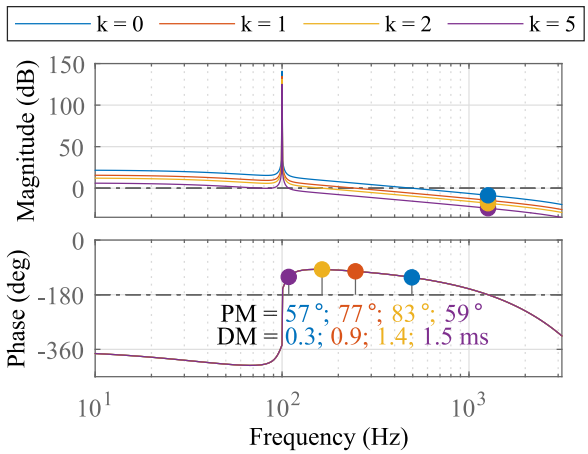

Fig. 11. Bode plot of the circulating current control open-loop transfer function.

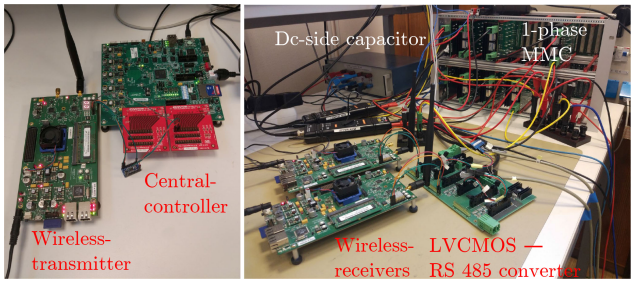

Fig. 12. Experimental setup: central controller and wireless transmitter (left), wireless receivers, submodules, and LVCMOS—RS 485 converter (right).

loops are stable with the end-to-end delay of the implemented setup with all the k values.

In wired communication experiments, T_{COM} components (b) and (c) are not present, and the total delay is 123.70 μs.

E. Experimental Results and Discussion

The experimental setup is shown in Fig. 12. The central controller and the submodules are roughly 2 m apart in a power electronics laboratory room. In order to obtain the packet loss characteristics of the wireless communication of the experimental setup, three measurements are done on wireless communication. Each of the measurements lasts 1 h. During the measurements, the MMC does not have dc-side voltage; the central controller transmits a fixed sinusoidal reference, while m_a is 0.95. The packet losses are determined from the first submodule controller of the upper arm. The statistics of the packet losses of the three measurements are shown in Table IV. The mean packet loss length is around 100 μs, which corresponds to a single packet loss. The maximum packet loss length and standard deviation notably changes between different measurements.

A set of experiments is conducted with the MMC while changing the controller parameters in Table II related to k and keeping any other setting. k is changed in the range 0–5. Note that, by setting $k = 5$, the MMC becomes immune to the packet losses within 5.45 standard deviation of the losses according to the results of measurement 2 in Table IV. The ac-side voltage and circulating current together with their harmonic spectra

TABLE IV
WIRELESS COMMUNICATION PACKET LOSS CHARACTERISTICS

	Meas. 1	Meas. 2	Meas. 3
Mean (μs)	101	104	91
Maximum (μs)	940	977	584
Standard deviation (μs)	59.8	73.3	30.8
Count	14840	14610	6835
Fraction of lost packets* $(\times 10^{-4})$	4.12	4.21	1.73

*Fractions of lost packets are calculated based on the mean, count values, and the total number of packages transmitted in an hour.

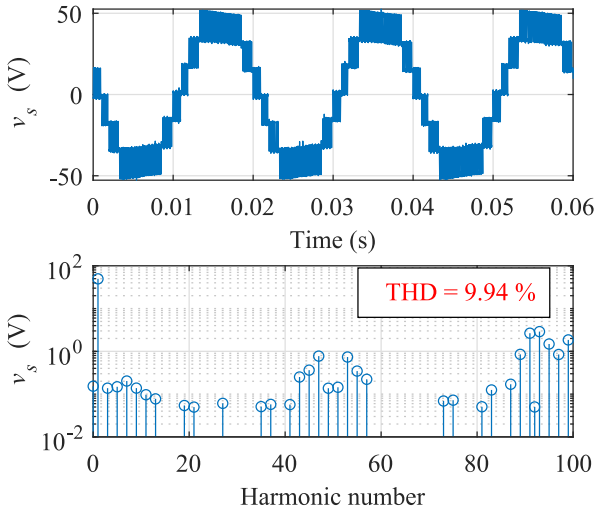

Fig. 13. AC-side voltage (upper) and harmonics spectrum (lower). The fundamental component peak value is 49.50 V.

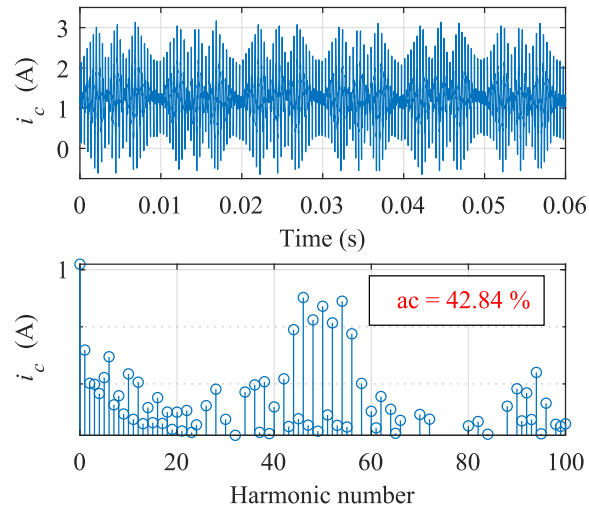

Fig. 14. Circulating current (upper) and harmonics spectrum (lower). The ac value corresponds to $I_{\mathrm{ac,rms}}/I_{\mathrm{dc}}$, including all the ac harmonics. DC is 1.25 A.

and one capacitor voltage in the steady state for $k = 5$ are shown in Figs. 13–15, respectively. The harmonic components are calculated based on "very short time harmonic measurements" in [50]. Harmonics larger than 0.1% of the fundamental component and up to the 100th harmonic are shown in the figures and included in the total harmonic distortion (THD) calculation. Figs. 13–15 show that the MMC operates stably with the proposed wireless control in the steady state. The dominant

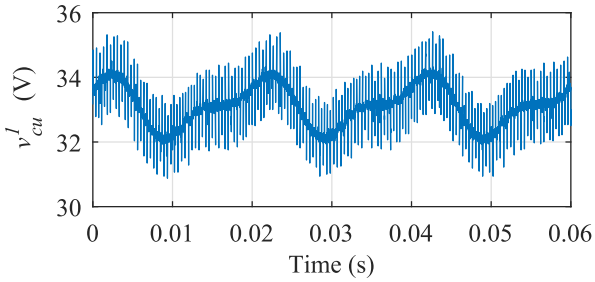

Fig. 15. Capacitor voltage of a submodule. The mean value is 33.12 V.

TABLE V
MMC PERFORMANCE WITH WIRELESS AND WIRED COMMUNICATION

	k	0	1	2	3	4	5
i	Wireless (%)	11.46	10.58	10.36	10.30	10.25	9.94
	Wired (%)	9.55	9.59	9.64	9.71	9.72	9.74
	Ratio	1.20	1.10	1.07	1.06	1.05	1.02
ii	Wireless (%)	41.98	43.08	43.51	44.25	44.15	42.84
	Wired (%)	45.72	45.31	45.07	43.99	43.81	43.88
	Ratio	0.92	0.95	0.97	1.01	1.01	0.98

switching harmonics in the ac-side voltage are around $2Nf_c$. There is no significant harmonic on/around f_c and its integer multiples except for the Nth multiples. This indicates the success of the proposed carrier synchronization method [42], [43]. The second and fourth harmonics in the circulating current are suppressed, and the dominant harmonics are around Nf_c. The capacitor voltage of a submodule is stable around its nominal value.

The experiments are repeated with the wired communication having the same controller parameters of the wireless case except for the compensation of T_d in the resonant controllers. In Table V, the performance of the MMC with wireless and wired control with different k values are compared. In the table, (i) and (ii), both in percent, correspond to the ac-side voltage THD and circulating current ac component ratio (the root mean square of all the ac harmonic components divided by the dc component, $I_{\mathrm{ac,rms}}/I_{\mathrm{dc}}$), respectively. The ratio in the table is wireless to wired. For wireless control and $k = 0$, in the ac-side voltage harmonic spectrum, there are higher low-frequency baseband harmonics (5, 7, 9, and the like) and slightly higher switching harmonics compared to the wired case. As the closed-loop control bandwidth decreases (k increases), the baseband and the switching harmonics of the wireless case approach those of the wired case. Consequently, while the ac-side voltage THD of wireless control is higher than that of the wired case for $k = 0$, it decreases and approaches the THD of the wired case as the closed-loop control bandwidth decreases.

The circulating current spectra of the wireless and wired cases have their dominant harmonics around Nf_c, as expected. However, for $k = 0$, the wireless case has higher wideband harmonics and lower dominant harmonics than the wired case. The dominant harmonics have a higher weight in the ac component calculation than the wideband harmonics. Hence, the ac component of the circulating current in wireless control is lower than the wired for $k = 0$. As the bandwidth decreases, the spectrum of the wireless control approaches that of the wired case as well as the ac component value.

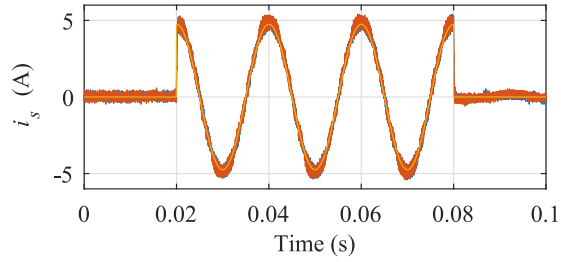

Fig. 16. AC-side current dynamic responses of the wired (blue), wireless (orange) cases, and $i_s^\star$ (yellow) overlapped. At 0.02 s, $\hat{i}_s^\star$ is stepped from 0 to 4.75 A and at 0.08 s, back to 0 A.

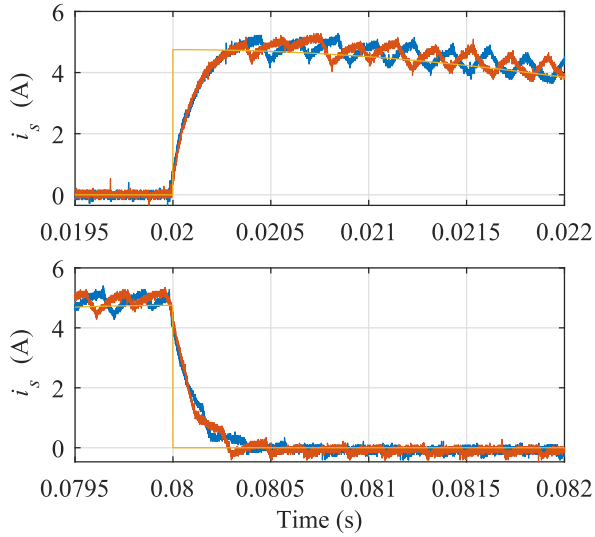

Fig. 17. Zoom-in views of the ac-side current dynamic responses of the wired (blue), wireless (orange) cases, and $i_s^\star$ (yellow) around the step times. At 0.02 s, $\hat{i}_s^\star$ is stepped from 0 to 4.75 A and at 0.08 s, back to 0 A.

The dynamic response of the wirelessly controlled MMC to step changes in the ac-side current reference is observed when $k = 5$. The ac-side current reference is defined in its controller (see Fig. 6) as

$$i_s^\star = \hat{i}_s^\star \sin(\omega_1 t + \phi) = \frac{V_{\mathrm{dc}}}{2} m_a \frac{1}{R_o} \sin(\omega_1 t + \phi) \qquad (9)$$

where $\hat{i}_s^\star$ is the peak value of $i_s^\star$. $\hat{i}_s^\star$ is adjusted by changing m_a while keeping R_o constant, as defined in Table I. At 0.02 s, $\hat{i}_s^\star$ is stepped up from 0 to 4.75 A (corresponding to m_a stepped from 0 to 0.95) with ϕ being $\pi/2$ so that at the instant of the step, the peak current is demanded. At 0.08 s, $\hat{i}_s^\star$ is stepped back to 0 A. The experiment is repeated with wired control for transient performance comparison. The ac-side current waveform of the wireless and wired control cases and $i_s^\star$ are shown in Fig. 16. The three waveforms overlap finely. The zoom-in views of the waveforms around the step times are shown in Fig. 17. Wireless and wired cases have similar transient responses. They have a quick initial response and converge to $i_s^\star$ in 300 μs with the help of the feedforward. Both the steady-state and dynamic results verify the viability of the wireless control of MMC submodules and show that it can perform comparably to the wired control.

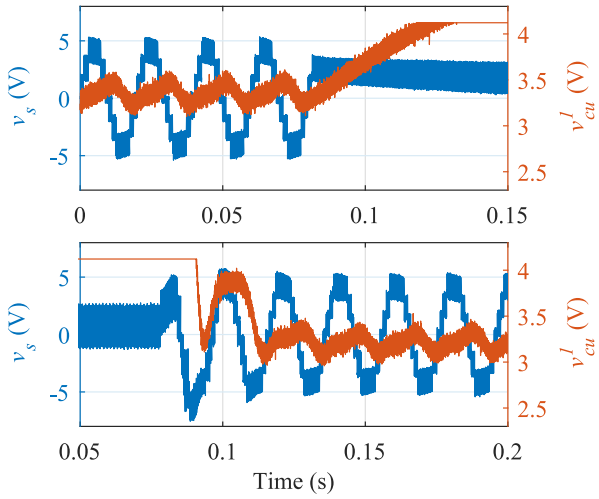

Fig. 18. AC-side voltage (blue) and a single submodule capacitor voltage (orange) just before (top) and right after (bottom) two different 2.68 s single train of packet losses.

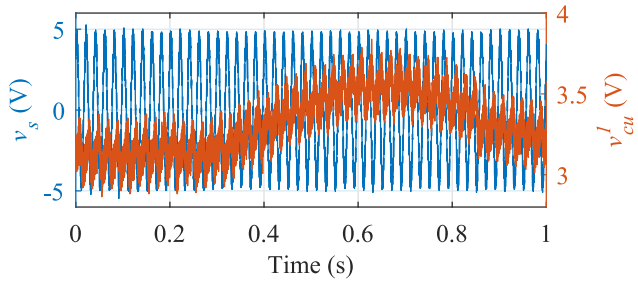

Fig. 19. AC-side voltage (blue) and a single submodule capacitor voltage (orange) during a periodic train of packet losses. Every third packet is transmitted.

As a further study, long packet loss trains are generated artificially in wireless communication, and the stability and performance of the MMC are observed. These experiments are carried out with 10-V dc-side voltages for the safety of the setup. Two cases of packet loss are experimented with: single train and periodic trains. During the loss trains, none of the submodules receives wireless data.

The single train is experimented with up to 2.68 s (26 800 consecutive losses). In this case, the submodules operate like a dc-to-dc converter. They provide a fixed voltage on the ac side depending on the last successively received insertion index. As the communication is recovered, the submodules continue their operation successfully. However, having a constant insertion index disturbs submodule capacitor voltage balancing. In the case of long packet loss intervals, and if there is no other measure taken, the submodule capacitors may get charged above their voltage ratings, as shown in Fig. 18.

Periodic trains are implemented such that after one successful wireless transmission, communication is disabled for some interval. Then, the cycle repeats. It is observed that if the closed-loop current control bandwidth is decreased as in (3), then the MMC might operate stably up to the communication disable interval with the k value used for the calculation of controller parameters. However, if the periodic loss trains occur such that the synchronization flag is always missed, then the MMC suffers from the problems related to the asynchrony of the carriers and overcharge/discharge of the submodule capacitor voltages. As an example, in Fig. 19, every third wireless packet is transmitted, and the submodule capacitor voltage is not in a steady state.

V. Conclusion and Future Work

Wireless control of MMC submodules may offer cheaper converter stations, reduced installation time, and higher converter availability. However, it comes with fundamental operational challenges due to its higher latency and lower reliability than the wired control. In this article, for the first time, a wireless MMC control approach is proposed, analyzed, and verified experimentally. The control is based on the distributed architecture with broadcast type of wireless communication. Even with an elementary wireless network with no measures for higher reliability, the wireless control performs comparably to the wired control with high closed-loop control bandwidth in the steady state. As the bandwidth decreases, the two methods perform similarly. They also have similar transient responses. The proposed control approach can be taken as the basis for the wireless control of an industrial-scale MMC. For this aim, several other technical, implementation, and financial aspects need to be studied, which are beyond the scope of this article. The technical aspects include higher reliability of the MMC with the autonomous operation of the submodules in cases of wireless communication errors that persist beyond the considered tolerable packet loss train. Also, a low-latency high-reliability wireless network designed for industrial control systems can be exploited. Furthermore, fault-handling algorithms suitable for wireless communication should be established. The implementation aspects are related to the installation and realization of wireless control in an industrial-scale MMC station, some of which are mentioned in Section I. These aspects include but are not limited to the proper installation of the wireless network in MMC stations, the viability of the wireless communication in the EMI environment of MMCs, the security of the wireless network, and monitoring tasks.

Acknowledgment

The authors would like to thank Dr. Luca Bessegato, Dr. Panagiotis Bakas, and Anant Narula for the design and construction of the components of laboratory-scale MMC used in the experiments.

References

[1] A. Lesnicar and R. Marquardt, "An innovative modular multilevel converter topology suitable for a wide power range," in *Proc. IEEE Bologna Power Tech Conf.*, 2003, vol. 3, pp. 1–6.

[2] T. Westerweller, K. Friedrich, U. Armonies, A. Orini, D. Parquet, and S. Wehn, "Trans bay cable—World's first HVDC system using multilevel voltage-sourced converter," in *Proc. Cigré Session*, 2010, pp. 1–6.

[3] ABB, *Why HVDC?* Accessed on: Apr. 24, 2020. [Online]. Available: https://new.abb.com/systems/hvdc/why-hvdc

[4] A. Willig, K. Matheus, and A. Wolisz, "Wireless technology in industrial networks," *Proc. IEEE*, vol. 93, no. 6, pp. 1130–1151, Jun. 2005.

[5] M. Wollschlaeger, T. Sauter, and J. Jasperneite, "The future of industrial communication: Automation networks in the era of the Internet of things and Industry 4.0," *IEEE Ind. Electron. Mag.*, vol. 11, no. 1, pp. 17–27, Mar. 2017.

[6] Y. Peng, W. Qiao, L. Qu, and J. Wang, "Sensor fault detection and isolation for a wireless sensor network-based remote wind turbine condition monitoring system," *IEEE Trans. Ind. Appl.*, vol. 54, no. 2, pp. 1072–1079, Mar./Apr. 2018.

[7] O. Kreibich, J. Neuzil, and R. Smid, "Quality-based multiple-sensor fusion in an industrial wireless sensor network for MCM," *IEEE Trans. Ind. Electron.*, vol. 61, no. 9, pp. 4903–4911, Sep. 2014.

[8] Z. Hamici and W. Abu Elhaija, "Novel current unbalance estimation and diagnosis algorithms for condition monitoring with wireless sensor network and internet of things gateway," *IEEE Trans. Ind. Inform.*, vol. 15, no. 11, pp. 6080–6090, Nov. 2019.

[9] S. K. Mazumder, R. Huang, and K. Acharya, "Rotor position feedback over an RF link for motor speed control," *IEEE Trans. Power Electron.*, vol. 25, no. 4, pp. 907–913, Apr. 2010.

[10] V. Roscher *et al.*, "Synchronisation using wireless trigger-broadcast for impedance spectroscopy of battery cells," in *Proc. IEEE Sensors Appl. Symp.*, 2015, pp. 1–6.

[11] T. Gherman, M. Ricco, J. Meng, R. Teodorescu, and D. Petreus, "Smart integrated charger with wireless BMS for EVs," in *Proc. 44th Annu. Conf. IEEE Ind. Electron. Soc.*, 2018, pp. 2151–2156.

[12] K. Acharya, M. Tahir, and S. K. Mazumder, "Communication fault-tolerant wireless network control of a load-sharing multiphase interactive power network," in *Proc. 37th IEEE Power Electron. Spec. Conf.*, 2006, pp. 1–8.

[13] A. Alfergani, A. Khalil, and Z. Rajab, "Networked control of AC microgrid," *Sustain. Cities Soc.*, vol. 37, pp. 371–387, Feb. 2018.

[14] H. Liang, B. J. Choi, W. Zhuang, and X. Shen, "Stability enhancement of decentralized inverter control through wireless communications in microgrids," *IEEE Trans. Smart Grid*, vol. 4, no. 1, pp. 321–331, Mar. 2013.

[15] Q. Shafiee, Č. Stefanović, T. Dragičević, P. Popovski, J. C. Vasquez, and J. M. Guerrero, "Robust networked control scheme for distributed secondary control of islanded microgrids," *IEEE Trans. Ind. Electron.*, vol. 61, no. 10, pp. 5363–5374, Oct. 2014.

[16] S. K. Mazumder, K. Acharya, and M. Tahir, ""Wireless" control of spatially distributed power electronics," in *Proc. 20th Annu. IEEE Appl. Power Electron. Conf. Expo.*, 2005, vol. 1, pp. 75–81.

[17] S. K. Mazumder, M. Tahir, and S. L. Kamisetty, "Wireless PWM control of a parallel DC-DC buck converter," *IEEE Trans. Power Electron.*, vol. 20, no. 6, pp. 1280–1286, Nov. 2005.

[18] C. Batard, G. Andrieux, N. Ginot, and M. A. Mannah, "Wireless transmission of IGBT driver control," in *Proc. 24th Annu. IEEE Appl. Power Electron. Conf. Expo.*, 2009, pp. 1257–1262.

[19] Y. M. Lai, S. C. Tan, and Y. M. Tsang, "Wireless control of load current sharing information for parallel-connected DC/DC power converters," *IET Power Electron.*, vol. 2, no. 1, pp. 14–21, Jan. 2009.

[20] D. Li and C. N. Man Ho, "Master-slave control of parallel-operated interfacing inverters based on wireless digital communication," in *Proc. IEEE Energy Convers. Congr. Expo.*, 2018, pp. 1466–1472.

[21] K. Sharifabadi, L. Harnefors, H.-P. Nee, S. Norrga, and R. Teodorescu, *Design Control and Application of Modular Multilevel Converters for HVDC Transmission Systems*. Chichester, U.K.: Wiley–IEEE Press, 2016.

[22] *IEEE Guide for Control Architecture for High Power Electronics (1 MW and Greater) Used in Electric Power Transmission and Distribution Systems*, IEEE Standard 1676-2010, 2011.

[23] J. M. Guerrero, M. Chandorkar, T. Lee, and P. C. Loh, "Advanced control architectures for intelligent microgrids—Part I: Decentralized and hierarchical control," *IEEE Trans. Ind. Electron.*, vol. 60, no. 4, pp. 1254–1262, Apr. 2013.

[24] H. Han, X. Hou, J. Yang, J. Wu, M. Su, and J. M. Guerrero, "Review of power sharing control strategies for islanding operation of AC microgrids," *IEEE Trans. Smart Grid*, vol. 7, no. 1, pp. 200–215, Jan. 2016.

[25] K. Rajesh, S. Dash, R. Rajagopal, and R. Sridhar, "A review on control of AC microgrid," *Renewable Sustain. Energy Rev.*, vol. 71, pp. 814–819, May 2017.

[26] M. H. Andishgar, E. Gholipour, and R. Hooshmand, "An overview of control approaches of inverter-based microgrids in islanding mode of operation," *Renewable Sustain. Energy Rev.*, vol. 80, pp. 1043–1060, Dec. 2017.

[27] Y. Zhou, D. Jiang, P. Hu, J. Guo, Y. Liang, and Z. Lin, "A prototype of modular multilevel converters," *IEEE Trans. Power Electron.*, vol. 29, no. 7, pp. 3267–3278, Jul. 2014.

[28] B. Xia *et al.*, "Decentralized control method for modular multilevel converters," *IEEE Trans. Power Electron.*, vol. 34, no. 6, pp. 5117–5130, Jun. 2019.

[29] M. A. Parker, L. Ran, and S. J. Finney, "Distributed control of a fault-tolerant modular multilevel inverter for direct-drive wind turbine grid interfacing," *IEEE Trans. Ind. Electron.*, vol. 60, no. 2, pp. 509–522, Feb. 2013.

[30] B. P. McGrath, D. G. Holmes, and W. Y. Kong, "A decentralized controller architecture for a cascaded H-bridge multilevel converter," *IEEE Trans. Ind. Electron.*, vol. 61, no. 3, pp. 1169–1178, Mar. 2014.

[31] P.-H. Wu, Y.-C. Su, J.-L. Shie, and P.-T. Cheng, "A distributed control technique for the multilevel cascaded converter," *IEEE Trans. Ind. Appl.*, vol. 55, no. 2, pp. 1649–1657, Mar./Apr. 2019.

[32] Y. Park, J. Yoo, and S. Lee, "Practical implementation of PWM synchronization and phase-shift method for cascaded H-bridge multilevel inverters based on a standard serial communication protocol," *IEEE Trans. Ind. Appl.*, vol. 44, no. 2, pp. 634–643, Mar./Apr. 2008.

[33] A. The, C. Bruening, and S. Dieckerhoff, "CAN-based distributed control of a MMC optimized for low number of submodules," in *Proc. IEEE Energy Convers. Congr. Expo.*, 2015, pp. 1590–1594.

[34] L. Mathe, P. D. Burlacu, and R. Teodorescu, "Control of a modular multilevel converter with reduced internal data exchange," *IEEE Trans. Ind. Inform.*, vol. 13, no. 1, pp. 248–257, Feb. 2017.

[35] S. Yang, Y. Tang, and P. Wang, "Distributed control for a modular multilevel converter," *IEEE Trans. Power Electron.*, vol. 33, no. 7, pp. 5578–5591, Jul. 2018.

[36] K. Ilves, A. Antonopoulos, S. Norrga, and H.-P. Nee, "A new modulation method for the modular multilevel converter allowing fundamental switching frequency," *IEEE Trans. Power Electron.*, vol. 27, no. 8, pp. 3482–3494, Aug. 2012.

[37] A. Antonopoulos, L. Ängquist, and H.-P. Nee, "On dynamics and voltage control of the modular multilevel converter," in *Proc. 13th Eur. Conf. Power Electron. Appl.*, 2009, pp. 1–10.

[38] L. Ängquist, A. Antonopoulos, D. Siemaszko, K. Ilves, M. Vasiladiotis, and H.-P. Nee, "Open-loop control of modular multilevel converters using estimation of stored energy," *IEEE Trans. Ind. Appl.*, vol. 47, no. 6, pp. 2516–2524, Nov./Dec. 2011.

[39] K. Ilves, L. Harnefors, S. Norrga, and H.-P. Nee, "Analysis and operation of modular multilevel converters with phase-shifted carrier PWM," *IEEE Trans. Power Electron.*, vol. 30, no. 1, pp. 268–283, Jan. 2015.

[40] P. Dan Burlacu, L. Mathe, and R. Teodorescu, "Synchronization of the distributed PWM carrier waves for modular multilevel converters," in *Proc. Int. Conf. Optim. Elect. Electron. Equip.*, 2014, pp. 553–559.

[41] C. L. Toh and L. E. Norum, "A high speed control network synchronization jitter evaluation for embedded monitoring and control in modular multilevel converter," in *Proc. IEEE Grenoble Conf.*, 2013, pp. 1–6.

[42] B. Ciftci, J. Gross, S. Norrga, L. Kildehøj, and H.-P. Nee, "A proposal for wireless control of submodules in modular multilevel converters," in *Proc. 20th Eur. Conf. Power Electron. Appl.*, 2018, pp. 1–10.

[43] S. Yang, H. Wang, H. Chen, W. Song, and T. Wang, "Probability-based modeling and analysis for PS-PWM in an MMC distributed control system with sub-module asynchrony," *IEEE Trans. Power Electron.*, vol. 34, no. 11, pp. 10392–10397, Nov. 2019.

[44] *IEEE Standard for Telecommunications and Information Exchange Between Systems—LAN/MAN Specific Requirements—Part 11: Wireless Medium Access Control (MAC) and Physical Layer (PHY) Specifications: High Speed Physical Layer in the 5 GHz Band*, IEEE Standard 802.11a-1999, 1999.

[45] C. Wang, L. Xiao, H. Jiang, and T. Cai, "Analysis and compensation of the system time delay in an MMC system," *IEEE Trans. Power Electron.*, vol. 33, no. 11, pp. 9923–9936, Nov. 2018.

[46] S. Buso and P. Mattavelli, *Digital Control in Power Electronics*, 2nd ed. San Rafael, CA, USA: Morgan & Claypool, 2015.

[47] A. Willig, M. Kubisch, C. Hoene, and A. Wolisz, "Measurements of a wireless link in an industrial environment using an IEEE 802.11-compliant physical layer," *IEEE Trans. Ind. Electron.*, vol. 49, no. 6, pp. 1265–1282, Dec. 2002.

[48] L. Bessegato, A. Narula, P. Bakas, and S. Norrga, "Design of a modular multilevel converter prototype for research purposes," in *Proc. 20th Eur. Conf. Power Electron. Appl.*, 2018, pp. 1–10.

[49] L. Corradini and P. Mattavelli, "Modeling of multisampled pulse width modulators for digitally controlled DC-DC converters," *IEEE Trans. Power Electron.*, vol. 23, no. 4, pp. 1839–1847, Jul. 2008.

[50] *IEEE Recommended Practice and Requirements for Harmonic Control in Electric Power Systems*, IEEE Standard 519–2014, 2014.

Barış Çiftçi (Student Member, IEEE) was born in Nazilli, Turkey, in 1987. He received the B.Sc. and M.Sc. degrees in electrical and electronics engineering from Middle East Technical University, Ankara, Turkey, in 2011 and 2014, respectively. He is currently working toward the Ph.D. degree with the KTH Royal Institute of Technology, Stockholm, Sweden.

From 2011 to 2017, he was a Design Engineer and Systems Engineer with Aselsan, Ankara. His research interests include wireless control of modular multilevel converter submodules.

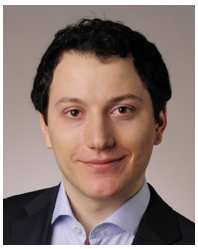

Sebastian Schiessl (Member, IEEE) received the Dipl.-Ing. degree in electrical engineering from the Technical University of Munich, Munich, Germany, in 2012, and the Ph.D. degree from the KTH Royal Institute of Technology, Stockholm, Sweden, in 2019.

In his thesis, conducted at the Department of Information Science and Engineering, he analyzed the queueing delay of ultra-reliable low-latency wireless communication systems based on finite-blocklength information theory. He then remained at the KTH Royal Institute of Technology to work on a project on edge computing applications, focusing on software-defined radio implementation for both IEEE 802.11 and 4G/LTE systems. In January 2020, he joined u-blox Athens S.A., Maroussi, Greece, to work on the standardization of vehicle-to-everything communication systems within the IEEE 802.11 working group.

James Gross (Senior Member, IEEE) received the Ph.D. degree from Technische Universität Berlin, Berlin, Germany, in 2006.

From 2008 to 2012, he was with RWTH Aachen University as an Assistant Professor and a Research Associate of RWTH's Center of Excellence on Ultra-High Speed Mobile Information and Communication. Since November 2012, he has been with the School of Electrical Engineering and Computer Science, KTH Royal Institute of Technology, Stockholm, Sweden, where he is currently a Professor of Machine-to-Machine Communications. At KTH Royal Institute of Technology, he was the Director for the ACCESS Linnaeus Centre from 2016 to 2019, while he is currently an Associate Director in the newly formed KTH Digital Futures Research Center, as well as Co-Director in the newly formed VINNOVA Competence Center on Trustworthy Edge Computing Systems and Applications. He is a Co-Founder of R3 Communications GmbH, a Berlin-based venture capital-backed company in the area of ultra reliable low-latency wireless networking for industrial automation. He has authored more than 150 (peer-reviewed) papers in international journals and conferences. His research interests include mobile systems and networks, with a focus on critical machine-to-machine communications, edge computing, resource allocation, as well as performance evaluation.

Dr. Gross is the recipient of the Best Paper Awards at the 2015 ACM International Conference on Modeling, Analysis, and Simulation of Wireless and Mobile Systems, the 2009 IEEE International Symposium on a World of Wireless, Mobile, and Multimedia Networks, and the European Wireless 2009. He was the recipient of the ITG/KuVS Dissertation Award for his Ph.D. thesis in 2007.

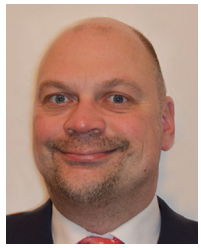

Lennart Harnefors (Fellow, IEEE) received the M.Sc., Licentiate, and Ph.D. degrees in electrical engineering from the KTH Royal Institute of Technology, Stockholm, Sweden, in 1993, 1995, and 1997, respectively, and the Docent (D.Sc.) degree in industrial automation from Lund University, Lund, Sweden, in 2000.

From 1994 to 2005, he was with Mälardalen University, Västerås, Sweden, as a Professor of Electrical Engineering. From 2001 to 2005, he was, in addition, a part-time Visiting Professor of electrical drives with the Chalmers University of Technology, Göteborg, Sweden. In 2005, he joined ABB, HVDC Product Group, Ludvika, Sweden, where, among other duties, he led the control development of the first generation of multilevel-converter HVdc light. In 2012, he joined ABB, Corporate Research, Västerås, where he became a Senior Principal Scientist in 2013. He is also, a part-time Adjunct Professor of power electronics with the KTH Royal Institute of Technology. His research interests include control and dynamic analysis of power electronic systems, particularly grid-connected converters and ac drives.

Dr. Harnefors is an Editor for the IEEE JOURNAL OF EMERGING AND SELECTED TOPICS IN POWER ELECTRONICS and an Associate Editor for the *IET Electric Power Applications*. He was the recipient of the 2020 IEEE Modeling and Control Technical Achieved Award and was acknowledged as an Outstanding Reviewer for the IEEE TRANSACTIONS OF POWER ELECTRONICS in 2018.

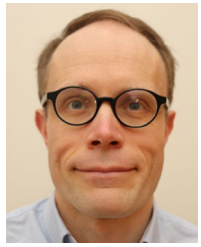

Staffan Norrga (Member, IEEE) was born in Lidingö, Sweden, in 1968. He received the M.Sc. degree in applied physics from the Linköping Institute of Technology, Linköping, Sweden, in 1993, and the Ph.D. degree in electrical engineering from the KTH Royal Institute of Technology, Stockholm, Sweden, in 2005.

From 1994 to 2011, he was a Development Engineer with ABB, Västerås, Sweden, in various power-electronics-related areas such as railway traction systems and converters for HVdc power transmission systems. He is currently an Associate Professor in Power Electronics with the KTH Royal Institute of Technology. He is the inventor or co-inventor of more than ten granted patents and has authored or coauthored more than 100 scientific papers published at international conferences or in journals. His research interests include power electronics and its applications in power grids, renewables, and electric vehicles.

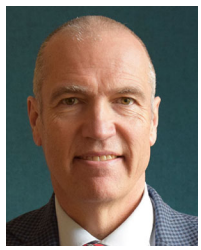

Hans-Peter Nee (Fellow, IEEE) was born in Västerås, Sweden, in 1963. He received the M.Sc., Licentiate, and Ph.D. degrees in electrical engineering from the KTH Royal Institute of Technology, Stockholm, Sweden, in 1987, 1992, and 1996, respectively.

Since 1999, he has been a Professor of Power Electronics with the Department of Electrical Engineering, KTH Royal Institute of Technology. His research interests include power electronic converters, semiconductor components, and control aspects of utility applications, such as flexible ac transmission systems, high-voltage dc transmission, and variable-speed drives.

Dr. Nee was a member of the Board of the IEEE Sweden Section for several years and was the Chair of the Board from 2002 to 2003. He is also a member of the European Power Electronics and Drives Association and is involved with its Executive Council and International Steering Committee.